Korean J. Chem. Eng., **28**(1), 272-278 (2011)
DOI: 10.1007/s11814-010-0352-y

Preparation of C/C composites by the chemical vapor infiltration (CVI) of propane pyrolysis

Kyung-Hoon Bang*, Gui-Yung Chung*†, and Hyung-Hoi Koo**

*Department of Chemical Engineering, Hong-Ik University, 72-1 Sangsudong, Mapoku, Seoul 121-791, Korea
**ADD, Yuseong P. O. Box 35-5, Daejeon 305-600, Korea
(*Received 6 May 2010 • accepted 10 June 2010*)

Abstract−The preparation of C/C composites by the chemical vapor infiltration (CVI) of the pyrolysis carbon from propane was studied. Pyrolysis carbon was deposited at 30 torr and at temperatures between 1,173 and 1,233 K. The rate of carbon deposition increased slightly with time. The main gas products in the exit gas were methane, ethylene, and acetylene. The fraction of ethylene decreased and that of acetylene increased with the reaction temperature and the propane concentration. The produced propyl radicals reacted further at a high temperature and at a high propane concentration. These trends were similar to those of the reported data. Changes of the shapes of deposited carbon in the pores of preform were confirmed with SEM photos. The mathematical modeling of the system with the deposition rate constant from the reference estimated experimental data well.

Key words: CVI, Propane, Pyrolysis Carbon, C/C Composites, Rate of Deposition

INTRODUCTION

C/C composites have good properties such as thermal and corrosion resistance. The shortcomings that carbon matrices are broken easily are compensated by reinforcing with fibers and making composite materials by chemical vapor infiltration (CVI). In this process how the preforms are filled with deposited carbon uniformly without any remaining pores is the main concern of many researchers. CVI originated in efforts to densify porous graphite bodies by infiltration of carbon [1]. The earliest use of CVI was the infiltration of fibrous alumina with chromium carbide. Since then this technique has developed commercially and many carbon-carbon composites have been produced by CVI.

The pyrolysis of hydrocarbons such as methane [2], propylene [3], and propane [4] has been studied extensively. Murphy et al. [5] studied the thermal decompositions of many hydrocarbons at high temperatures between 1,173 and 1,373 K. Methane, ethylene, acetylene, propane and neopentane have been pyrolyzed in a flow system, and the volatile pyrolysis products were analyzed. Eleven aromatic hydrocarbons, containing 14 or fewer carbon atoms, accounted for 98+% of the liquid products recovered in each case. Benzene was the main product followed by naphthalene. Acetylene was found to be a major component of the gaseous effluent. It was proposed that acetylene may be a common factor in the pyrolysis of aliphatic hydrocarbons, perhaps acting as the precursor of both surface carbon and aromatic hydrocarbons by a process of head to tail linkage of two carbon units at active surface sites to form chains that then undergo dehydrogenation to carbon or cyclization and desorption as aromatic species.

Pyrolysis of propane like that of many other hydrocarbons leads to hundreds of species and reactions [6-8]. Fig. 1 is the reaction mechanisms of the pyrolysis of propane. Firstly, methyl, ethyl, and n- & i-propyl radicals are produced. Then the gas products, such as methane, ethylene and acetylene, are generated [9,10]. Benzene and toluene are also produced.

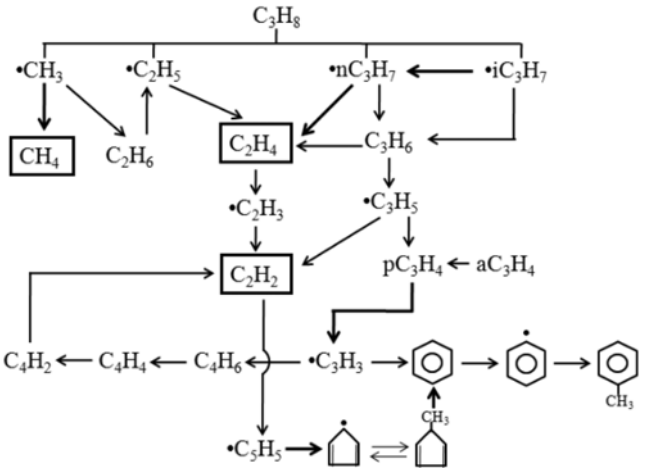

Fig. 1. Reaction mechanisms of the pyrolysis of propane at 1,248 K. The main gas products detected in this research are methane, ethylene and acetylene. The reaction paths for the production of big molecules were simplified. Details are in the references 9-11.

Ziegler et al. [10-12] had identified carbon/carbon composite synthesis involves the deposition of a matrix of pyrocarbon produced by the pyrolysis of a gaseous hydrocarbon in a preform made of carbon fibers. They carried out the pyrolysis of propane in a wide range of temperature (1,173-1,298 K) with a residence time of 1 s. The pyrolysis generates various gaseous species such as hydrogen, various light hydrocarbons, aromatic and polyaromatic hydrocarbon species (PAH). Khan et al. [13] also pyrolyzed propane in a

†To whom correspondence should be addressed.
E-mail: gychung@hongik.ac.kr

Table 1. The experimental conditions used in our research and in the references

	Conditions in this research	Conditions in the experiments by Ziegler et al. [12]	Conditions in the experiments by Khan et. al. [13]
% of propane	100%	12.9%% in N_2	0.5% in N_2
Temperature [K]	1,173-1,233	1,173-1,298	913-1,283
Partial pressure of propane [torr]	30	2.6	6
Total pressure [torr]	30	20	1,216
Flow rate of propane [cc/min]	30	5	12.5
Reactor volume [cm^3]	1,250	90	190
Residence time [s]	25	1	1.8

flow reactor system at temperatures ranging from 913 to 1,283 K. The products of pyrolysis were collected and analyzed.

As shown in Table 1, Ziegler et al. [12] used 12.96% of propane in nitrogen at 2.625 torr. On the other hand, Khan et al. [13] used 0.5% propane in nitrogen of 12.5 cc/min at 6 torr. In this research, pure propane was used and effects of the propane concentration were observed.

Modeling of the manufacturing of fiber-reinforced ceramic composites by CVI was studied by many researchers. Gases diffuse into the void regions and react to produce solid deposits. Numerical simulations were used to optimize parameters of CVI processes. In the research of CVI of SiC, it was assumed that an overall deposition reaction is the first order on the reactant concentration and the surface area available for deposition [14,15]. The same assumptions were used in this research.

The process of the preparation of C/C composites by the chemical vapor infiltration (CVI) of pyrolysis carbon was studied in this research. This work describes the experimental and modeling studies of the formation of pyrocarbon obtained by the pyrolysis of propane at 1,173-1,233 K. Pyrolysis carbon was deposited on the lateral surfaces of carbon fibers in the layered preform. The amount of deposited carbon and the compositions of the exit gas after the deposition reaction were measured and compared with the reported data. The mathematical modeling of the system has been done with the deposition rate constant from the reference [16]. Time changes of the amount of deposition were estimated and compared with the experimental data. Changes of the shapes of deposited carbon in the pores of preform were confirmed with SEM photos.

MODEL DEVELOPMENT

The cylindrical preform is composed of layers of woven fabrics. Fibers in the preform are assumed nonporous. It is also assumed that pores distributed evenly in the whole preform as shown in Fig. 2.

The reactant gas, i.e., propane, flows from one side of the preform to another in the isothermal reactor. For the gas concentration distribution, a pseudo-steady state was assumed. It is supposed that propane infiltration reaction is a first-order reaction of propane by which 1 mole of propane creates 3 mole bulk carbon [17].

$$C_3H_8 \rightarrow 3C+4H_2 \quad (1)$$

There is a z-directional convection in the pores among fibers. The mole balances of each ingredient were also made.

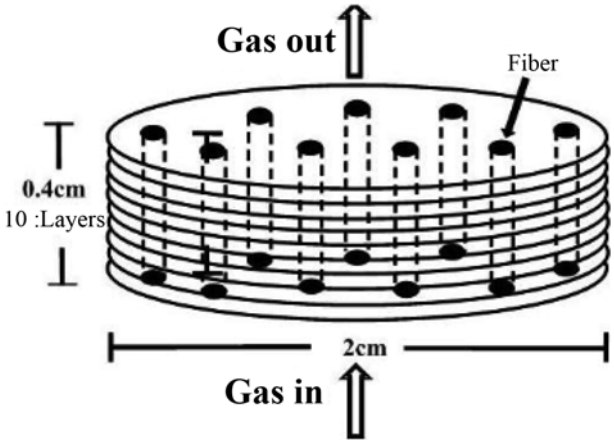

Fig. 2. Schematic diagram of the preform used in the numerical modeling.

$$\frac{1}{A}\frac{\partial QC_A}{\partial z} - 2\nu_A \pi W k r_f C_A = 0 \quad (2)$$

Here, A [cm^2] is the cross-sectional area of the preform, C_A [mol·cm^3] the concentration of propane, W [cm^{-2}] the number of fibers per unit cross-sectional area of the preform, r_f [cm] the radius of fiber, k [cm·s^{-1}] the first order deposition rate constant, ν_A the stoichiometric coefficient in Eq. (1). The first term in Eq. (2) is the change of propane due to a convectional gas flow and the second one is that due to a deposition on the lateral surfaces of cylindrical fibers.

Vaidyaraman et al. [16] reported the rate constant for carbon deposition from propane as follows.

$$\ln(k_s) = 2.2 - 23{,}610/RT \quad (3)$$

Here, k_s [cm·s^{-1}] is the rate constant for deposition on the surface, R the gas constant [cal·$gmol^{-1}K^{-1}$], and T [K] the reaction temperature. They obtained the activation energy as 23.6 kcal·mol^{-1} which is much lower than the 48-60 kcal·mol^{-1} reported in the literature [18]. They mentioned that the discrepancy might be due to the scattered data and the uncertainty of the concentration near the hot side.

The momentum balance equation for packed columns was used for the calculation of pressure distribution. Changes of a fiber radius with time were calculated with the following equation.

$$\frac{\partial r_{fz}}{\partial t} = \frac{qM_m}{\rho_m} k C_{A,z} \quad (4)$$

Here, q is the mole number of deposited C from one mole of pro-

pane, M_m and ρ_m are the molecular weight and the density of deposited pyrolysis C, respectively. The amount of deposition per unit cross-sectional area of the preform for the preform thickness of Δz is expressed as follows.

$$D_z = \pi \sum_{z=0}^{L} (r_{fz}^2 - r_{fo}^2) \Delta z W \rho_m \quad (5)$$

The porosity ε_z is obtained in a similar way.

$$\varepsilon_z = 1 - \pi r_{fz}^2 W \quad (6)$$

With the dimensionless parameters such as $\sigma(=r_f/r_{fo})$ and $\xi(=z/H)$, equations were changed into a dimensionless form and calculated in the finite difference method. Calculations were carried out after the length in the z-direction was divided into 20 elements.

Porosity at z was calculated first and then pressure, P_z, total concentration, C_z, and volumetric flow rate, Q_z, were calculated. With these values, the mole fraction of propane was calculated. The fiber radius, r_{fz}, the amount of infiltration, D_z, and the porosity, ε_z, were calculated. Calculations were terminated when pores were plugged.

EXPERIMENTAL

As shown in Fig. 3, the experimental settings are composed of gas supply parts, furnace, and gas exhaust parts. A horizontal cylindrical electrical furnace was used. A cylindrical graphite tube in the quartz tube was positioned in the center of the heating section of the furnace to prevent the deposition of carbon on the wall of the quartz tube. The preform and the thermocouple were also positioned in the center of the heating section of the furnace. The carbon fiber preforms (20×20×4 mm) made of layered woven fabrics were used.

The experimental procedures were as follows. The carbon preform was dried and weighted. This preform in the graphite tube was positioned at the center of the tube furnace. The reactor was evacuated and then heated while helium gas passed through. As the temperature of the furnace reached 1,173 K, 30 cc/min of propane was injected at 30 torr. After the deposition reaction, propane was switched to argon and the reactor was cooled down. The exhaust gas was analyzed with a gas chromatograph during the reaction. The preforms after deposition were weighted and SEM photos of them were taken.

The depositions of pyrolysis carbon from propane were carried

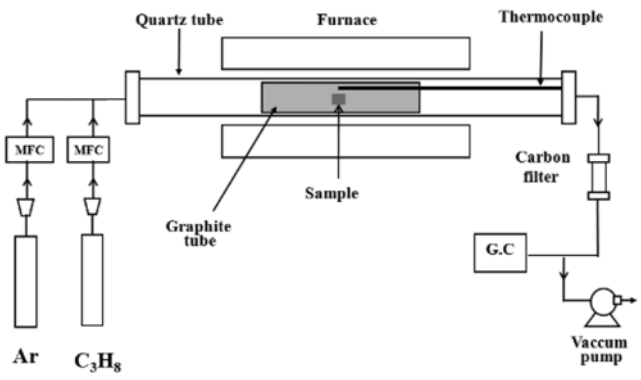

Fig. 3. Schematic diagram of the experimental setting.

Table 2. Dimensions of the preform used in the experiment

Preform size	20 mm×20 mm×4 mm
Surface area	0.28 m^2/g
Average pore diameter	12.8 nm
Initial porosity	80%

out at 1,173-1,233 K, 30 torr, and 30 cc/min of propane. The amounts of deposition were measured at 3, 6, 9, 12, and 18 hours. The deposition conditions and the physical properties of the layered carbon preform are in Table 2.

For the GC analysis of the exhaust gas, the Porapak N packed column and TCD were used. The injection and the detection temperatures were 200 °C. The oven temperature started at 40 °C initially, and increased 20 °C/min up to 190 °C. The residence times of the main products at our GC conditions were 1.4 min for methane, 4.7 min for ethylene, and 5.9 min for acetylene. The other products were not detected because of the small amounts.

RESULTS AND DISCUSSION

1. Effects of Temperature

Changes of the amount of deposition with time at different reaction temperatures are in Fig. 4. Dots are experimental data and lines are the fitting curves. At a constant temperature, the amount of deposition increased continuously with time. The slope of a curve at a certain point is the rate of deposition at that point. As time passed, the rate of deposition increased slightly due to the increasing surface area. This is explained in this way. The surface area is one of several driving forces for deposition. Here, the surface area is mainly the lateral surface area of fibers in the preform. Hence, the rate of deposition increases with the fiber diameters increasing due to deposition. As expected, the amount and the rate of deposition increased with the increasing temperature. Furthermore, it increased more between 1,203 and 1,233 K than did between 1,173 and 1,203 K.

Fig. 5 is the initial rate of deposition per unit hour and unit mass of the preform obtained with the graph in Fig. 4. When the experi-

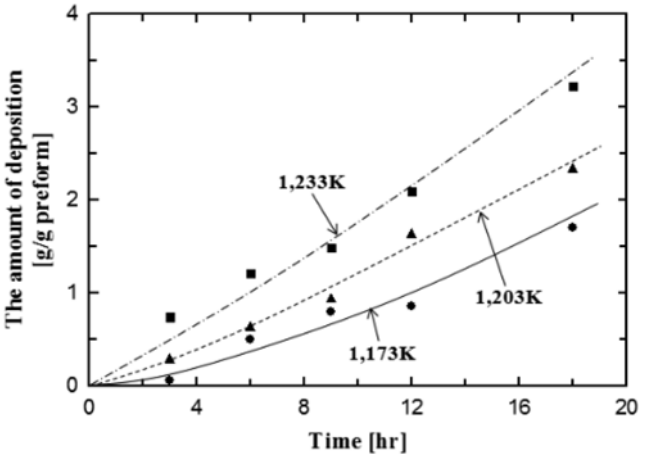

Fig. 4. Changes of the amount of deposition per unit mass of the preform as a function of deposition time at different reaction temperatures. The dotted and the solid lines are curves fitting the experimental data.

mental data of Ziegler et al. [12] were multiplied by 20, they matched with ours. This means that the rate of deposition in our research was 20 times fast. This can be explained with the concentration of propane. As shown in Table 1, the pure propane at 30 torr was used in our experiments. On the other hand, Ziegler et al. used 13% propane at 2.625 torr. The molar ratio of propane used in our experiment to that in Ziegler's experiment was almost 88. Because of this difference in the concentration, there appeared almost 20 times difference in the rate of deposition. Differences due to the other driving forces for deposition such as the initial surface area and the initial porosity of the preform could not be compared clearly because of the absence of data.

2. Changes of the Shapes of Deposits

As mentioned above, the amount of deposition increases with time in Fig. 4. The surface area is one of driving forces for deposition. Here, the surface area is mainly the lateral surface area of fibers in the preform. As deposition proceeds, the lateral area of fibers increases with the increase of fiber diameters. Hence, the rate of deposition increases. These phenomena can be shown in the changes of shapes of deposits in the preform.

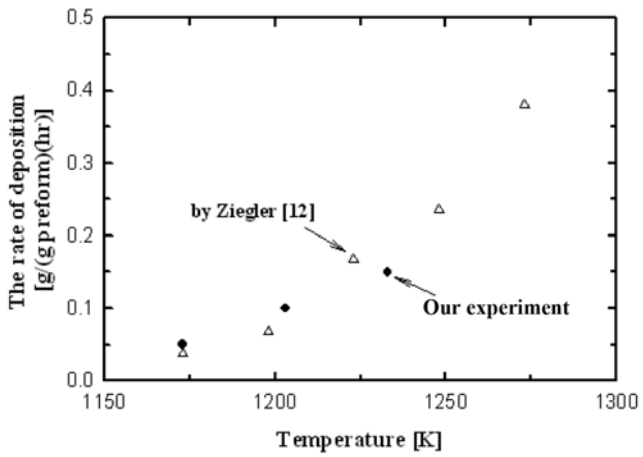

Fig. 5. Changes of the initial rate of deposition as a function of temperature. The triangles are the results obtained by multiplying the data of Ziegler et al. [12] by 20.

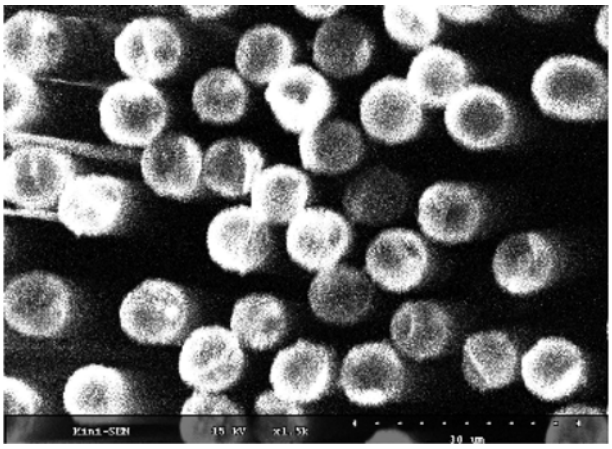

Fig. 6. SEM photograph (×1,500) of fibers in the preform before deposition.

Fig. 6 is the SEM photograph of fibers in the preform before deposition. The pores among fibers are very large and fibers have smooth lateral surfaces. How these pores are filled with the pyrolysis car-

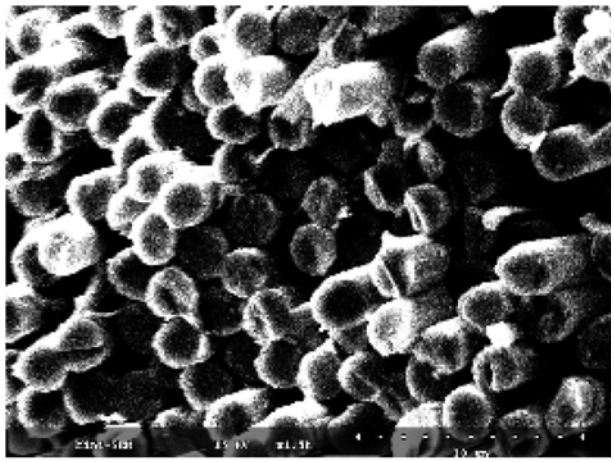

(a) 3 hrs

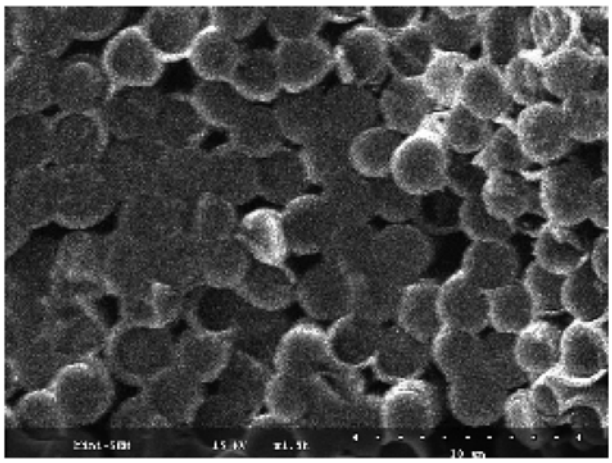

(b) 6 hrs

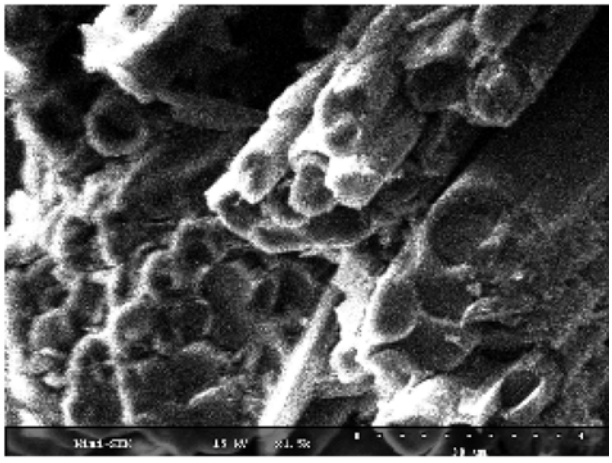

(c) 9 hrs

Fig. 7. SEM photographs (×1,500) of the C/C composites after the infiltration reactions for (a) 3 hrs (b) 6 hrs, and (c) 9 hrs at 1,203 K. Reaction conditions: 30 torr, and 30 cc/min C_3H_8.

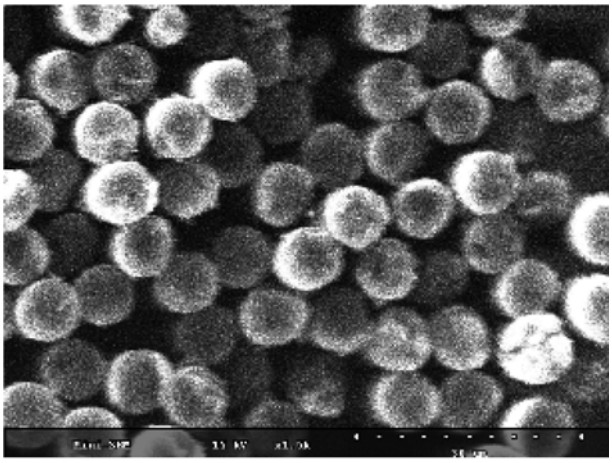

(a) at 1,173 K

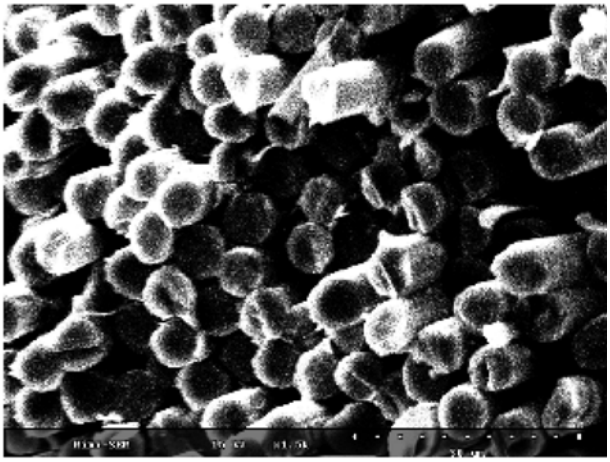

(b) at 1,203 K

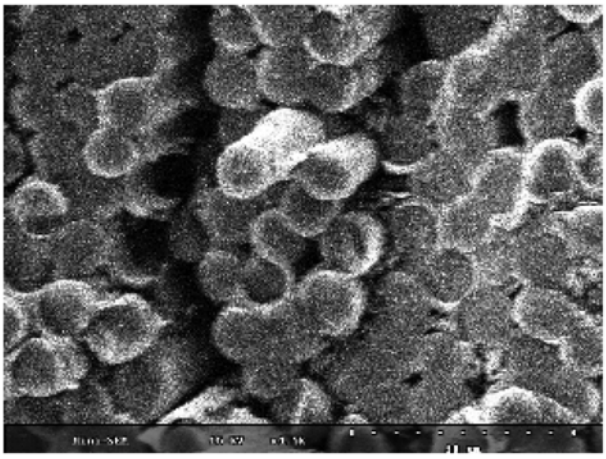

(c) at 1,233 K

Fig. 8. SEM photographs (×1,500) of the C/C composites after the infiltration reactions (a) at 1,173 K (b) at 1,203 K, and (c) at 1,233 K. Other reaction conditions: 3 hrs, 30 torr, and 30 cc/min C_3H_8.

bon by the CVI of propane are shown in Fig.'s 7(a)-(c). They are the SEM photos of C/C composites after the deposition reactions for 3, 6, and 9 hours. The fiber radii increased with the deposition time and the amounts of deposition on the lateral surfaces of fibers also did. Furthermore, it is clearly seen that pores among fibers are almost filled at 9 hour deposition.

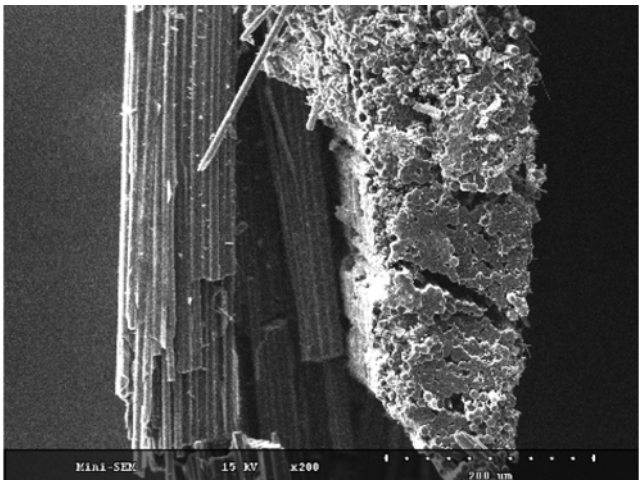

Fig. 9. SEM photograph (×200) of the C/C composite after the infiltration reaction for 9 hrs at 1,173 K, 30 torr, and 30 cc/min C_3H_8.

Additionally, the effects of reaction temperature on the shapes of deposits are shown in Fig. 8(a)-(c). There was not so much deposit on the lateral surfaces of fibers at 1,173 K in Fig. 8(a). However, there appeared a large amount of deposits, and the pores among fibers were almost filled with deposits at 1,203 and 1,233 K.

Fig. 9 is the photograph of fiber bundles deposited for 9 hours at 1,173 K. Even if a few cracks are shown, most of pores among fibers in the fiber bundles of the preform are filled with deposits.

3. Changes of the Compositions in the Exit Gas

Propane is decomposed thermally at a high temperature and produces many products. Ziegler et al. [12] and Kahn et al. [13] reported that the thermal decomposition of propane produces many kinds of products from light hydrocarbons to heavy hydrocarbons. The main products are methane, acetylene, and ethylene as shown in Fig. 1.

The compositions of these products at 1,173-1,278 K, measured with GC, are shown in Fig. 10(a)-(c). The methane composition slightly decreases with the reaction temperature. The ethylene composition decreases and the acetylene composition increases with the reaction temperature. The trends changing with temperature are similar with the experimental data reported by Ziegler et al. [12]. However, the fractions of methane and acetylene were quite big and those of ethylene were small compared to the data reported by Ziegler et al. [12]. These phenomena can be explained in the following way.

In the reaction paths shown in Fig. 1, propane decomposes first into methyl, ethyl, and propyl radicals. Then the methyl radicals change into methane. Additionally, the ethyl radicals change first into ethylene and then into acetylene by the separation of hydrogen. Following these reaction paths, it might be explained that the thermal decomposition of propyl radicals proceeds far and produces more acetylene at such a high concentration in our system. The concentrations and the pressures used in the experiments are shown in Table 1. The concentration of propane in our experiment

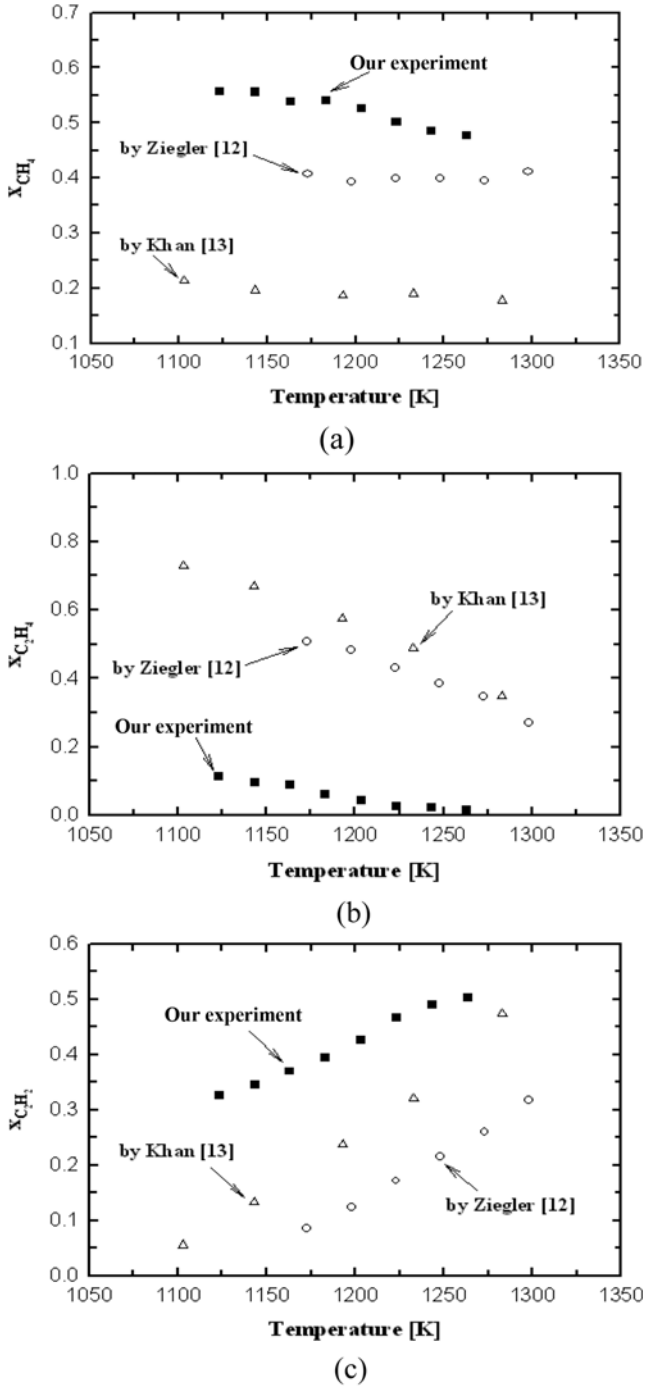

Fig. 10. Changes of the fractions of gas products such as (a) methane, (b) ethylene, and (c) acetylene with the reaction temperatures in the propane pyrolysis. Reaction conditions are 30 torr and 1,800 cc/hr. The circles are the data given by Ziegler et al. [12] and the triangles are the data given by Khan et al. [13].

is 88 times of that by Ziegler et al. [12] and 1,000 times of that by Kahn et al. [13]. The high concentration gave ethyl radicals more chances to collide with each other. As a result, more ethyl radicals could become acetylene. So the fraction of ethylene became small and that of acetylene quite big compared to the data reported by Ziegler [12] and Khan [13]. For the same reasons, the fraction of

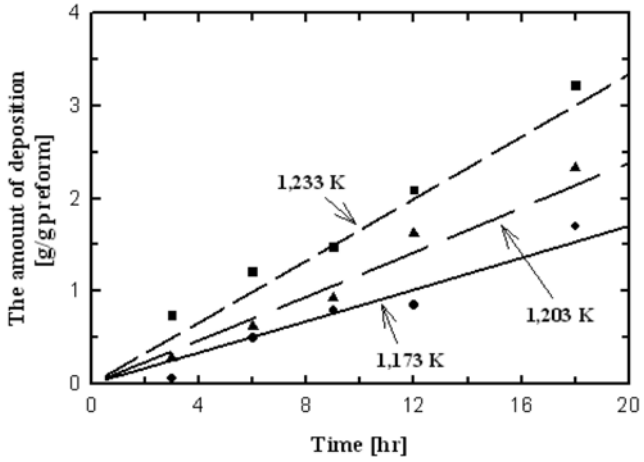

Fig. 11. Comparisons of the modeling calculations with the experimental data of the amount of deposition per unit mass of the preform. Modeling calculations were made with $0.7k_s$ at 1,173 K, k_s at 1,203 K, and $1.8k_s$ at 1,233 K. Here, k_s is the rate constant in Eq. (3).

methane became quite bigger than the data by Ziegler [12] and Khan [13].

The trends changing with temperature in Fig. 10 can be explained in the same way. At a high temperature, the reactions can go further, so ethylene decreases and acetylene increases.

4. The Numerical Simulation

The numerical simulations of the amount of deposition per unit mass of the preform at different temperatures are shown in Fig. 11. Dots are experimental results and curves are modeling simulations. Results of the modeling calculations estimated the experimental data well.

The rate constant, k_s, in Eq. (3) was used for the modeling calculations. As mentioned in the model development, Vaidyaraman et al. [16] reported the activation energy as 23.6 kcal·mol^{-1} which is lower than 48-60 kcal·mol^{-1} reported in the literature [18]. They mentioned that the discrepancy might be due to the scattered data and the uncertainty of the concentration near the hot side. However, the small activation energy reported by Vaidyaraman estimated our experimental data at 1,203 K well. On the other hand, when the rate constant was multiplied by 0.7 at 1,173 K and by 1.8 at 1,233 K, the modeling calculations fitted the experimental data well. A smaller rate constant was used at a low temperature and a bigger rate constant was used at a high temperature.

CONCLUSIONS

In this research, the process of the preparation of C/C composites by the chemical vapor infiltration (CVI) of propane was studied. Pyrolysis carbon was deposited on the lateral surfaces of carbon fibers in the layered preform. The amount of deposited carbon and the compositions of the exit gas after the deposition reaction were measured. And numerical simulations were carried out. The following conclusions were obtained.

1. The rate of deposition increased slightly with time due to the increasing surface area.

2. The main gas products in the exit gas were methane, ethyl-

ene, and acetylene. The fraction of ethylene decreased and that of acetylene increased with the reaction temperature and the propane concentration. The produced propyl radicals reacted further at a high temperature and at a high propane concentration. Even if it is not easy to compare different studies with different experimental conditions, the trends of the data are similar to those of the data reported in the references 12 and 13.

3. Changes of the shapes of deposited carbon in the pores of preform were confirmed with SEM photos. Most pores among fibers in the fiber bundles of the preform were filled with deposits.

4. The mathematical modeling of the system estimated the experimental data well with the deposition rate constant from reference 16.

ACKNOWLEDGEMENTS

This work was supported by the Korea Science and Engineering Foundation (KOSEF) grant (No. R01-2008-000-21103-0) funded by the Korean government. This research was also partially supported by the 2009 Hongik University Research Fund.

REFERENCES

1. P. Delhaes, *Carbon*, **40**, 641 (2002).
2. Z. Renjun, L. Qiangkun and L. Zhiyong, *J. Anal. Appl. Pyrol*., **13**(3), 183 (1988).
3. F. Billaud, *J. Anal. Appl. Pyrol.*, **21**(1/2), 15 (1991).
4. P. Dagaut, M. Cathonnet and J. C. Boettner, *Int. J. Chem. Kinet*, **24**, 813 (1992).
5. D. B. Murphy, R. W. Carroll and J. E. Klonowski, *Cabon*, **35**(12), 1819 (1997).
6. E. N. Wami, *Chem. Eng. Technol*., **17**, 195 (1994).
7. A. S. Tomlin, M. J. Pilling, J. H. Merkin, J. Brindley, N. Burgess and A. Gough, *Ind. Eng. Chem. Res*., **34**(11), 3749 (1995).
8. K. Norinaga and O. Deutschmann, *Ind. Eng. Chem. Res*., **46**(11), 3547 (2007).
9. C. Descamps, G. L. Vignoles, O. Fe´ron, F. Langlais and J. Lavenac, *J. Electrochem. Soc*., **148**(10), C695 (2001).
10. I. Ziegler, R. Fournet and P. M. Marquaire, *J. Anal. Appl. Pyrol.*, **73**, 212 (2005).
11. I. Ziegler, R. Fournet and P. M. Marquaire, *J. Anal. Appl. Pyrol.*, **73**, 231 (2005).
12. I. Ziegler, R. Fournet and P. M. Marquaire, *J. Anal. Appl. Pyrol.*, **79**, 268 (2007).
13. R. U. Khan, S. Bajohr, D. Buchholz, R. Reimert, H. D. Minh, K. Norinaga, V. M. Janardhanan, S. Tischera and O. Deutschmann, *J. Anal. Appl. Pyrol.*, **81**, 148 (2008).
14. G. Y. Chung, B. J. McCoy, J. M. Smith and D. E. Cagliostro, *AIChE J*., **39**(11), 1834 (1993).
15. M. S. Cho, J. W. Kim and G. Y. Chung, *Korean J. Chem. Eng*., **13**(5), 515 (1996).
16. S. Vaidyaraman, W. J. Lackey, and P. K. Agrawal, *Carbon*, **34**(5), 609 (1996).
17. I. Ziegler, R. Fournet and P. M. Marquaire, *J. Anal. Appl. Pyrol.*, **73**, 107 (2005).
18. P. A. Tesner, *Chemistry and physics of carbon*, Edited by P. A. Thrower, **9**, 173 (1973).